Celal Bayar University Journal of Science

Experimental and Theoretical Investigation of a new *β*-Diketiminate Derivative

İlkay Yıldırım[1]*

[1] Department of Radiotherapy, Vocational School, Biruni University, 34010 İstanbul, TURKEY
* iyildirim@biruni.edu.tr
* Orcid: 0000-0002-7423-5043

Received: 13 November 2020
Accepted: 2 June 2021
DOI: 10.18466/cbayarfbe.825395

Abstract

A new *β*-diketiminate compound (**I**) was synthesized, and its structure was determined by a single-crystal X-ray diffraction study. The molecule crystallizes as a salt in the monoclinic system, and the crystal structure is stabilized by intermolecular N─H···Cl hydrogen bonds. The structural and energetic properties were examined using the HSEH1PBE density functional method with cc-pvdz basis set. The optimized structure represents well the experimental structure. In addition, the noncovalent interactions have been also analyzed using Hirshfeld surface analysis. Hirshfeld surface analysis shows that H···H and H···Cl/Cl···H interactions contribute to about 94% of the total intermolecular interactions. Frontier molecular orbitals (HOMO-LUMO), their energy gap and associated parameters were determined.

Keywords: *β*-diketiminate, crystal structure, DFT, Hirshfeld surface.

1. Introduction

The *β*-diketiminate class, also known NacNac or [{ArNC(R)}$_2$CH]- (where Ar = aryl and R = Me or another organic group), occupies a rightful place among other ancillary supports, which applications change from structural inorganic/organometallic chemistry to bioinorganic systems and catalysis [1-4]. The *β*-diketiminate ligands are known to provide monoanionic, bidentate support for metal complexes and a high degree of steric control can be achieved depending on the choice of N-substituents [5]. The reactivity of these class of the ligands can also be improved significantly, by tuning the steric and electronic properties of the supporting *β*-diketiminate ligands [6,7].

Since the first such metal NacNac complexes were reported by McGeachin [8] and Holm [9], these ligand class has been often used to stabilize many elements in the periodic table and in unusual oxidation states [10]. A lot of complexes can be derived from variation of substituents on nitrogen atom of 1,3-diketimines by different hydrogen/alkyl/aryl/silyl/germanyl groups, as well metal ions [11-14]. Consequently, the resulting ligands become good σ donors and poor π acceptors like N-heterocyclic carbenes (NHCs), and thus have the potential to exhibit carbene-like chemistry.

In this paper, we report the synthesis and crystal structure of *N*-[(2*Z*,3*E*)-4-(isopropylamino)pent-3-en-2-ylidene]propan-2-aminium chloride salt (**I**) formed unexpectedly (Figure 1).

2. Materials and Methods

2.1. Synthesis

Two moles of $^{i}Pr_2$-nacnacH (1) (0.5 g) in 10 mL toluene were mixed with one mole of 1,2-bis(dimethylamino diborane dichloride (2) (0.248 g) in 5 mL toluene for 2 hours, and stand for two days. The precipitated colorless crystal (**I**) was filtered and washed cold ether. (Yield: % 48).

2.2. XRD Analysis

XRD data of **I** were collected at room temperature using a Mo K*α* radiation with STOE IPDS II diffractometer. During the process the *ω*-scan method was applied. X-AREA [15] and X-RED32 [15] were used to perform for data collection and cell refinement and for data reduction, respectively. Direct methods were used to solve the structure with SIR2019 [16]. Refinement of the structure was processed with SHELXL-2018 [17] on F^2 by means of the full matrix least-squares calculations. All of the H atoms bonded to C atoms were first located in Fourier difference maps then trade

as riding atoms, fixing the bond lengths at 0.93 Å for aromatic CH, 0.98 Å for methine CH and 0.96 Å for CH_3 atoms. Also, the H atoms bonded to N atoms were located from the Fourier-difference map but refined freely. All the details of the process are given in Table 1. The OLEX2 [18] was used to generate the molecular graphics.

The supplementary crystallographic data for the compound reported here is deposited at CCDC 2024442 and can be provided free of charge upon request to CCDC, 12 Union Road, Cambridge CB2 1EZ, UK [Fax: +44 1223 336 033, e-mail: deposit@ccdc.cam.ac.uk, https://www.ccdc.cam.ac.uk/structures/].

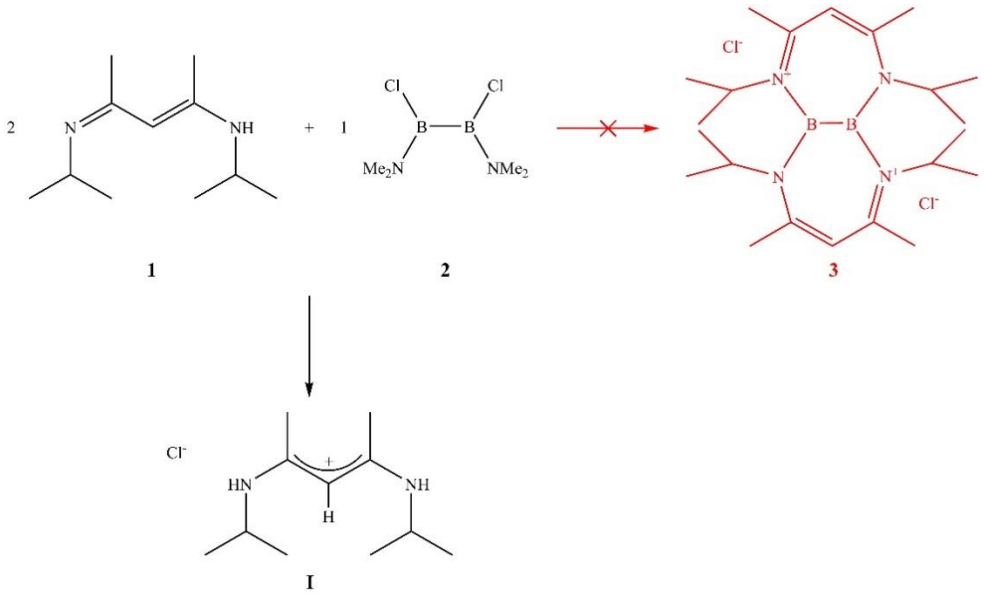

Figure 1. Chemical formula of **I**.

2.3. Computational Procedure

Theoretical calculations were carried out with the aid of GaussView 5 [19] molecular visualization software and Gaussian 09 program package [20]. The structural and other electronic properties of **I** were obtained using the HSEH1PBE density functional method [21-23] with cc-pvdz basis set [24]. The optimized geometry was confirmed to be real minima by frequency calculation (no imaginary frequencies).

3. Results and Discussion

To obtain dicationic bicyclic diborane derivative (**3**), 1,2-bis(dimethylamino)diborane dichloride (**2**) [25] was reacted with two equivalents $^{i}Pr_2$-nacnacH (**1**) [26] in toluene at room temperature. Unfortunately, desired product (3) could not be produced from the reaction. Presumably, compound **3** is very unstable so it immediately decomposes in the reaction media. By the diboran compound acts as reducing agent, imine group is converted to iminium cation salt through secondary amine group. Compound **I** is a decomposition product that is crystallized in a reaction mixture at room temperature. The compound **I** is stable in air atmosphere. Reaction was monitored by IR spectrum during the formation of compound **I**. In the spectrum, *β*-Diketimine (**1**) showed the bands at 3333 and 1648 cm^{-1} attributed to enamine and imine groups, respectively. Upon formation of iminium cation salt, the monitored bands at 3501 cm^{-1} and at 2085, 1593 cm^{-1} on the spectrum were attributed to secondary amine and iminium salt, respectively (Figure 2).

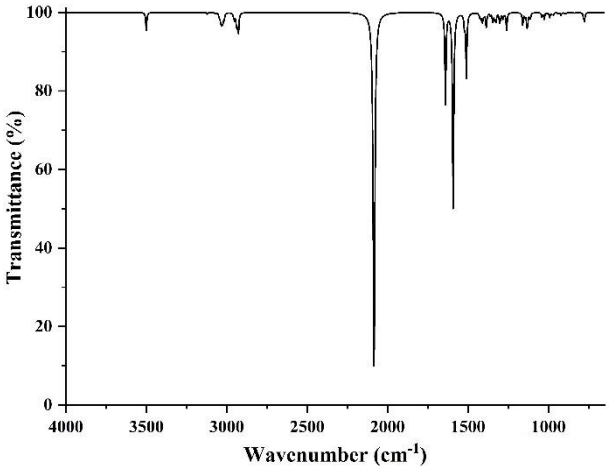

Figure 2. IR spectrum of **I.**

Celal Bayar University Journal of Science
Volume 17, Issue 3, 2021, p 297-304
Doi: 10.18466/cbayarfbe.825395

Table 1. Crystal data and structure refinement parameters for **I**.

CCDC depository	2024442
Color/shape	Colorless/prism
Chemical formula	$C_{11}H_{23}N_2^+ \cdot Cl^-$
Formula weight	218.76
Temperature (K)	296(2)
Wavelength (Å)	0.71073 Mo Kα
Crystal system	Monoclinic
Space group	$P2_1/c$ (No. 14)
Unit cell parameters	
a, b, c (Å)	11.6986(10), 11.9408(9), 19.8065(18)
α, β, γ (°)	90, 101.002(7), 90
Volume (Å^3)	2715.9(4)
Z	8
$D_{calc.}$ (g/cm^3)	1.070
μ (mm^{-1})	0.253
Absorption correction	Integration
$T_{min.}$, $T_{max.}$	0.8941, 0.9846
F_{000}	960
Crystal size (mm^3)	0.56 × 0.31 × 0.05
Diffractometer	STOE IPDS II
Measurement method	ω scan
Index ranges	$-13 \le h \le 13$, $-14 \le k \le 13$, $-23 \le l \le 23$
θ range for data collection (°)	$1.773 \le \theta \le 25.048$
Reflections collected	20101
Independent/observed reflections	4797/1949
$R_{int.}$	0.1543
Refinement method	Full-matrix least-squares on F^2
Data/restraints/parameters	4797/0/281
Goodness-of-fit on F^2	0.802
Final R indices [$I > 2\sigma(I)$]	R_1 = 0.0544, wR_2 = 0.0715
R indices (all data)	R_1 = 0.1646, wR_2 = 0.0928
$\Delta\rho_{max.}$, $\Delta\rho_{min.}$ (e/Å^3)	0.16, −0.16

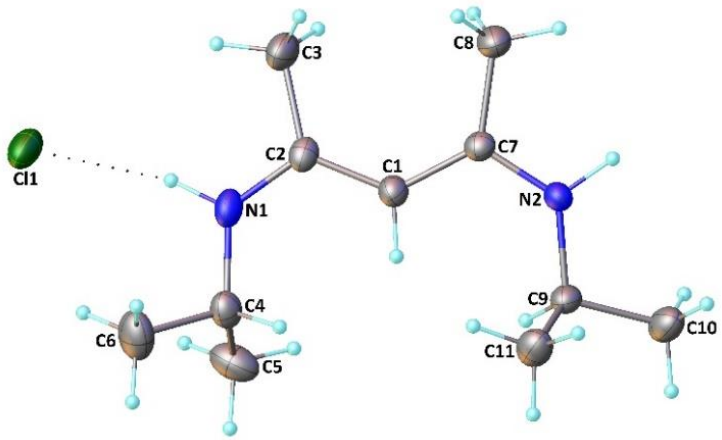

Figure 3. The molecular structure of one (A) of the two independent molecules present in the crystals of **I**. Dotted lines show the intermolecular H-bonding.

3.1. Experimental and Theoretical Structure

The solid-state structure of **I** has been unambiguously determined by single-crystal X-ray diffraction analysis (XRD), and its structural plot is presented in Figure 3, whilst some of the experimental and theoretical parameters are quoted in Table 2. Colorless crystals of **I** crystallize as a salt in the monoclinic system *P*21/*c* with two crystallographically independent molecules, A and B, in the asymmetric unit. In the following discussion, parameters related to the second molecule (B) are given in square brackets.

The compound is composed of an *N*-[(2*Z*,3*E*)-4-(isopropylamino)pent-3-en-2-ylidene]propan-2-aminium cation and one chloride anion. There are no chemically significant differences between the two cationic molecules in the asymmetric unit. The central C1─C2 and C1─C7 bond distances of 1.384(4) and 1.390(4) Å [1.389(4) and 1.380(4) Å], respectively, are almost equal to each other, and show an intermediate character between single (1.54 Å) and double bonds (1.34 Å) [27], indicating dispersion of positive charge over C2─C1─C7 atoms. These bonds were calculated at 1.432 and 1.380 Å, respectively. Although the N1─C4 and N2─C9 bond distances of 1.463(4) and 1.468(4) Å [1.469(4) and 1.463(4) Å], respectively, conform to a C─N single bond (1.48 Å), the N1─C2 and N2─C7 bond distances of 1.318(4) and 1.328(4) Å [1.327(4) and 1.332(4) Å], respectively, are shorter than a C─N single bond but longer than a C═N double bond (1.28 Å). These bonds were theoretically determined at 1.457, 1.455, 1.306 and 1.353 Å, respectively. So, this data suggests an extended electron delocalization over the N1─C2 and N2─C7 bonds since the C2─C3 and C7─C8 bond distances of 1.512(5) and 1.504(4) Å [1.498(4) and 1.495(4) Å] correspond to a C─C single bond, which were computed at 1.502 and 1.503 Å, respectively.

The molecular structure of **I** contains no intramolecular interactions. In the crystal structure, the cation is linked to the chloride anions by means of N─H···Cl hydrogen bonds, so forming $C_2^1(8)$ [28] chains along the c axis (Figure 4). Details of these interactions are given in Table 3.

Table 2. Selected geometric parameters for **I**.

Parameters	X-ray		DFT
	Molecule A	Molecule B	
Bond lengths (Å)			
N1─C2	1.318(4)	1.327(4)	1.306
N1─C4	1.463(4)	1.469(4)	1.457
N2─C7	1.328(4)	1.332(4)	1.353
N2─C9	1.468(4)	1.463(4)	1.455
C1─C2	1.384(4)	1.389(4)	1.432
C1─C7	1.390(4)	1.380(4)	1.380
C2─C3	1.512(5)	1.498(4)	1.502
C7─C8	1.504(4)	1.495(4)	1.503
Bond angles (°)			
C2─N1─C4	127.0(3)	126.6(3)	129.02
C7─N2─C9	126.8(3)	126.5(3)	127.25
N1─C2─C1	121.7(4)	122.0(3)	121.56
N1─C2─C3	114.1(3)	113.3(3)	114.03
N2─C7─C1	119.9(3)	120.5(3)	121.24
N2─C7─C8	114.8(3)	113.7(3)	113.10
C2─C1─C7	130.4(3)	129.6(3)	128.84
C1─C2─C3	124.3(3)	124.7(3)	124.39
C1─C7─C8	125.2(3)	125.8(3)	125.66
Torsion angles (°)			
C3─C2─N1─C4	−179.2(3)	−175.4(3)	179.13
C8─C7─N2─C9	−177.1(3)	177.3(3)	179.74
N1─C2─C1─C7	−172.4(3)	179.3(3)	−173.18
N2─C7─C1─C2	−177.9(4)	175.7(3)	−175.10
C2─C1─C7─C8	2.5(6)	−4.3(6)	4.32
C7─C1─C2─C3	8.9(6)	−0.9(6)	8.37

Celal Bayar University Journal of Science
Volume 17, Issue 3, 2021, p 297-304
Doi: 10.18466/cbayarfbe.825395

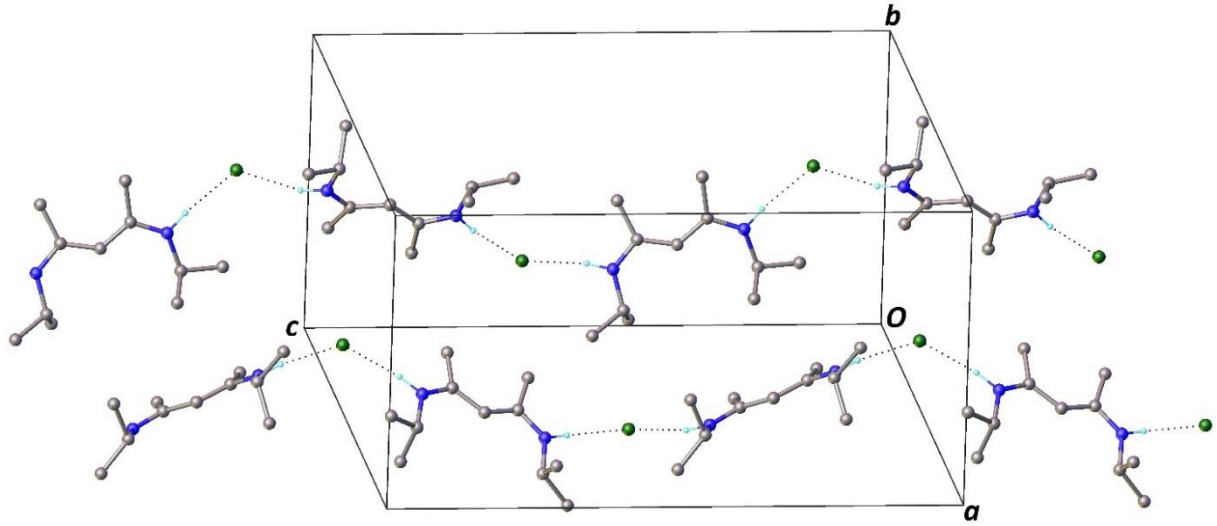

Figure 4. Part of the crystal structure of **I**, showing the formation of $C_2^1(8)$ chains along [001] built from N─H···Cl hydrogen bonds. For clarity, only H atoms involved in hydrogen bonding have been included.

Table 3. Hydrogen bonding geometry for **I**.

D─H···A	D─H (Å)	H···A (Å)	D···A (Å)	D─H···A (°)
N2A─H2A1···Cl1A^{i}	0.95(3)	2.32(3)	3.261(3)	171(3)
N2B─H2B1···Cl1B^{ii}	0.91(3)	2.32(4)	3.216(3)	170(3)
N1B─H1B1···Cl1B	0.98(4)	2.27(4)	3.240(3)	168(3)
N1A─H1A1···Cl1A	0.93(4)	2.32(4)	3.222(3)	163(3)

Symmetry codes: (i) *x*, −*y*+3/2, *z*−1/2; (ii) *x*, −*y*+1/2, *z*−1/2.

3.2. Hirshfeld Surface (HS) Analysis

HS analysis is very useful to picturize and examine important intra- or intermolecular interactions within the crystal structure.

The distance external to the surface d_e measures the distance between a surface to the neighboring nucleus while the distance internal to the surface d_i measures the distance between a surface to nearest atom in the molecule itself. The two-dimensional (2D) fingerprint plots based on HS analysis can provide the contributions of each specific contact pairs to HS [29]. The 2D fingerprint plots for **I** were generated by Crystal Explorer 17.5 program [30] and shown in Figure 5.

The fingerprint plots show that the main intermolecular interactions in **I** are H···H and H···Cl/Cl···H. The highest contribution to the total Hirshfeld surface occurs due to H···H close contacts with 73.2%. The proportion of H···Cl/Cl···H interactions comprises 20.2% of the surface. These intermolecular contacts correspond to about 94% of all noncovalent interactions. Missing percentages are H···C/C···H 4.9% and H···N/N···H 1.7% contacts.

3.3. Energetics and Stability

One way to get an idea on how compound interacts with other species is to analyze the highest occupied molecular orbital (HOMO) and the lowest unoccupied molecular orbital (LUMO) which are frontier molecular orbitals. In many reactions, electrons located in HOMO are donated first while a compound accepts electrons to its LUMO. Thus, one can easily measure chemical hardness, reactivity and many more parameters from the energy gap (ΔE) between HOMO and LUMO [31]. The global chemical reactivity descriptors (GCRD) such as the absolute electronegativity [$\chi = (I+A)/2$], the chemical potential [$\mu = -(I+A)/2$], the absolute hardness [$\eta = (I-A)/2$], softness ($S = 1/2\eta$) and electrophilicity index ($\omega = \mu^2/2\eta$) were calculated by taking the energies of HOMO as ionization potential ($I = -E_{HOMO}$) and LUMO as electron affinity ($A = -E_{LUMO}$) according to Koopmans Theorem [32].

Celal Bayar University Journal of Science
Volume 17, Issue 3, 2021, p 297-304
Doi: 10.18466/cbayarfbe.825395

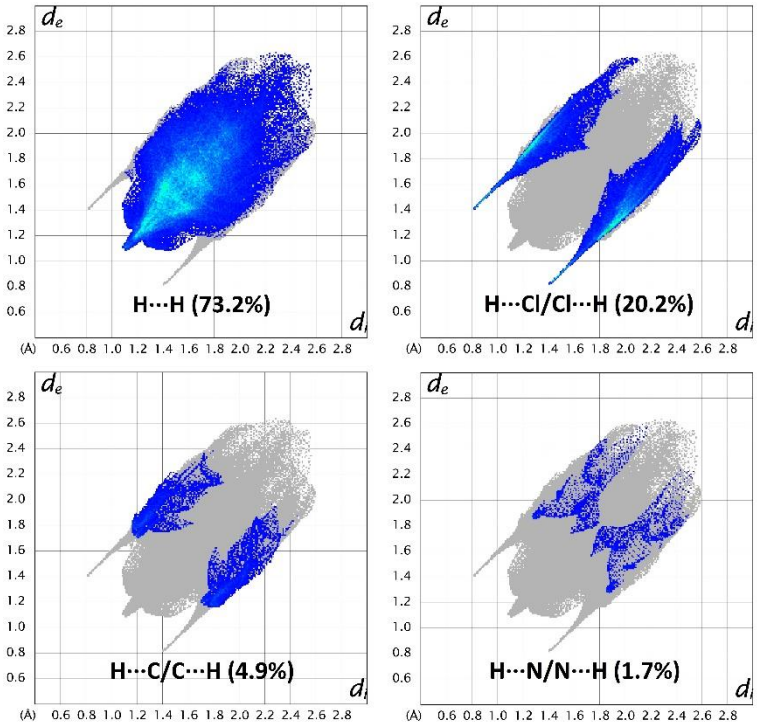

Figure 5. The 2D fingerprint plots with decomposition of dominant types of the intermolecular contacts of **I**.

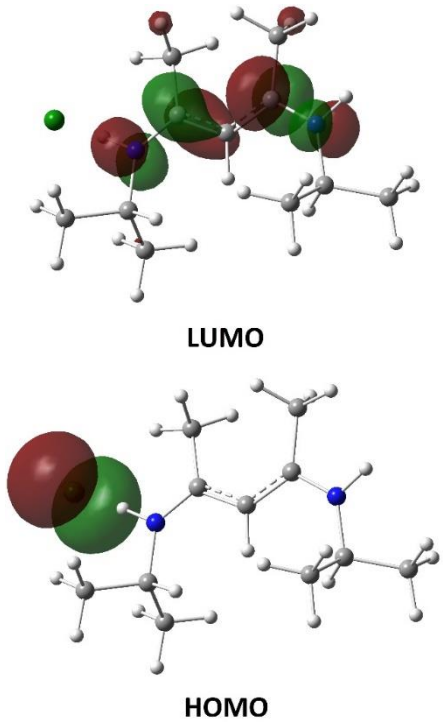

Figure 6. Frontier molecular orbital surfaces of compound **I**.

The contour plot of HOMO and LUMO orbitals of **I** is shown in Figure 6 while the GCRDs values are collected in Table 4. The calculated E_{HOMO}, E_{LUMO} and ΔE energies are 4.92, 1.85 and 3.07 eV, respectively. If the molecule is hard, the larger ΔE corresponds to the more hardness molecule. In this case, the compound has higher kinetic stability and thus, lower chemical reactivity. The molecules are kinetically stable with the hardness and chemical potential values of 1.54 and −3.39 eV, respectively. The other parameters such as softness (0.33 eV^{-1}), electronegativity (3.39 eV), and electrophilic index (3.73 eV) also suggest that the compound holds stability and chemical strength.

Table 4. Calculated energy values of **I**.

E_{HOMO} (eV)	−4.92
E_{LUMO} (eV)	−1.85
Energy gap (ΔE) (eV)	3.07
Electronegativity (χ) (eV)	3.39
Chemical potential (μ) (eV)	−3.39
Chemical hardness (η) (eV)	1.54
Chemical softness (S) (eV^{-1})	0.33
Electrophilicity index (ω) (eV)	3.73

4. Conclusion

In summary, compound **I** is investigated by using XRD and computational methods. Theoretical geometric parameters are in good agreement with the experimental findings. XRD results indicate that the compound crystallizes as a salt. The intermolecular N─H···Cl interactions are responsible for the stabilization of the crystal structure. In an effort to investigate the intermolecular interactions, HS

analysis was also carried out. The contributions of total HS were analyzed by plotting the fingerprint plots. The highest contribution of total HS was found as H···H: 73.2% and H···Cl/Cl···H: 20.2%. The calculated descriptors related to chemical reactivity showed a high energy gap between HOMO and LUMO which concluded that the compound has high kinetic stability and shows low intramolecular charge transfer and low chemical reactivity.

Acknowledgement

The support of Dr. Erkan FIRINCI is appreciated. In addition, for the X-ray data collection, I would like to thank to the support of the Crystallography Laboratory Unit supported by the University Research Fund (Project No: PYO.FEN.1906.19.001) from Ondokuz Mayıs University. I also thank Amasya University for providing the access to GaussView 5.0 and Gaussian 09W software packages.

Author's Contributions

İlkay Yıldırım: Drafted and wrote the manuscript, performed the experiment and result analysis.

Ethics

There are no ethical issues after the publication of this manuscript.

References

1. Dindar, S, Kharat, AN, Safarkoopayeh, B, Abbasi, A. 2021. Ruthenium (II) *β*-diketimine as hydroamination catalyst, crystal structure and DFT computations. *Transition Metal Chemistry*; 46(5): 403-413.

2. Rinke, P, Görls, H, Kretschmer, R. 2021. Calcium and Magnesium Bis(*β*-diketiminate) Complexes: Impact of the Alkylene Bridge on Schlenk-Type Rearrangements. *Inorganic Chemistry*; 60(7): 5310-5321.

3. Zhu, L, Xu, Y, Yuan, D, Wang, Y, Yao, Y. 2021. Synthesis and structural characterization of lanthanide monoborohydride complexes supported by 2-tertbutylphenyl substituted *β*-diketiminate, and their application in the ring-opening polymerization of lactide. *Journal of Organometallic Chemistry*; 934(15): 121662.

4. Li, B, Yang, Y, Zhu, H, Roesky, HW. 2021. (*β*-Diketiminato)aluminum hydroxides and the chalcogenide derivatives: Precursors for homo- and heterometallic complexes with Al-E-M (E = chalcogen, M = metal) frameworks. *Coordination Chemistry Reviews*; 429(15): 213625.

5. Zhong, M, Sinhababu, S, Roesky, HW. 2020. The unique *β*-diketiminate ligand in aluminum(I) and gallium(I) chemistry. *Dalton Transactions*; 49(5): 1351-1364.

6. Jones, C. 2017. Dimeric magnesium(I) *β*-diketiminates: a new class of quasi-universal reducing agent. *Nature Reviews Chemistry*; 1: 0059.

7. McWilliams, SF, Holland, PL. 2015. Dinitrogen Binding and Cleavage by Multinuclear Iron Complexes. *Accounts of Chemical Research*; 48(7): 2059-2065.

8. McGeachin, SG. 1968. Synthesis and properties of some *β*-diketimines derived from acetylacetone, and their metal complexes. *Canadian Journal of Chemistry*; 46(11): 1903-1912.

9. Parks, JE, Holm, RH. 1968. Synthesis, solution stereochemistry, and electron delocalization properties of bis(*β*-iminoamino)nickel(II) complexes. *Inorganic Chemistry*; 7(7): 1408-1416.

10. Tsai, Y-C. 2012. The chemistry of univalent metal *β*-diketiminates. *Coordination Chemistry Reviews*; 256(5-8): 722-758.

11. Liddle, ST, Arnold, PL. 2007. Synthesis and characterisation of yttrium complexes supported by the *β*-diketiminate ligand $\{ArNC(CH_3)CHC(CH_3)NAr\}^-$ (Ar = 2,6-$Pr^i_2C_6H_3$). *Dalton Transactions*; 30: 3305-3313.

12. Xiao, X, Hao, X, Bai, J, Chao, J, Cao, W, Chen, X. 2016. Synthesis, mechanism and ethylene polymerization catalysis of Ge(iv), Sn(ii) and Zr(iv) complexes derived from substituted *β*-diketiminates. *RSC Advances*; 6(65): 60723-60728.

13. Xiong, Y, Yao, S, Kostenko, A, Driess, M. 2018. An isolable *β*-diketiminato chlorosilylene. *Dalton Transactions*; 47(7): 2152-2155.

14. Bourget-Merle, L, Lappert, MF, Severn, JR. 2002. The chemistry of *β*-diketiminatometal complexes. *Chemical Reviews*; 102(9): 3031-3066.

15. X-AREA (version 1.18) and X-RED32 (version 1.04), Stoe & Cie, Darmstadt, Germany, 2002.

16. Burla, MC, Caliandro, R, Carrozzini, B, Cascarano, GL, Cuocci, C, Giacovazzo, C, Mallamo, M, Mazzone, A, Polidori, G. 2015. Crystal structure determination and refinement viaSIR2014. *Journal of Applied Crystallography*; 48(1): 306-309.

17. Sheldrick, GM. 2015. Crystal structure refinement with SHELXL. *Acta Crystallographica Section C: Structural Chemistry*; 71(1): 3-8.

18. Dolomanov, OV, Bourhis, LJ, Gildea, RJ, Howard, JAK, Puschmann, H. 2009. OLEX2: a complete structure solution, refinement and analysis program. *Journal of Applied Crystallography*; 42(2): 339-341.

19. Dennington, R, Keith, T, Millam, J. GaussView, Version 5, Semichem Inc., Shawnee Mission KS, 2009.

20. Frisch, MJ, Trucks, GW, Schlegel, HB, Scuseria, GE, Robb, MA, Cheeseman, JR, Scalmani, G, Barone, V, Mennucci, B, Petersson, GA, Nakatsuji, H, Caricato, M, Li, X, Hratchian, HP, Izmaylov, AF, Bloino, J, Zheng, G, Sonnenberg, JL, Hada, M, Ehara, M, Toyota, K, Fukuda, R, Hasegawa, J, Ishida, M, Nakajima, T, Honda, Y, Kitao, O, Nakai, H, Vreven, T, Montgomery, JA, Jr, Peralta, JE, Ogliaro, F, Bearpark, M, Heyd, JJ, Brothers, E, Kudin, KN, Staroverov, VN, Kobayashi, R, Normand, J, Raghavachari, K, Rendell, A, Burant, JC, Iyengar, SS, Tomasi, J, Cossi, M, Rega, N, Millam, NJ, Klene, M, Knox, JE, Cross, JB, Bakken, V, Adamo, C, Jaramillo, J, Gomperts, R, Stratmann, RE, Yazyev, O, Austin, A J, Cammi, R, Pomelli, C, Ochterski, J W, Martin, RL, Morokuma, K, Zakrzewski, VG, Voth, GA, Salvador, P, Dannenberg, JJ, Dapprich, S, Daniels, AD, Farkas, Ö,

Foresman, JB, Ortiz, JV, Cioslowski, J, Fox, DJ. Gaussian 09, Revision C.01, Gaussian, Inc., Wallingford CT, 2009.

21. Heyd, J, Scuseria, GE. 2004. Assessment and validation of a screened Coulomb hybrid density functional. *Journal of Chemical Physics*; 120(16): 7274-7280.

22. Heyd, J, Scuseria, GE. 2004. Efficient hybrid density functional calculations in solids: Assessment of the Heyd–Scuseria–Ernzerhof screened Coulomb hybrid functional. *Journal of Chemical Physics*; 121(3): 1187-1192.

23. Heyd, J, Peralta, JE, Scuseria, GE, Martin, RL. 2005. Energy band gaps and lattice parameters evaluated with the Heyd-Scuseria-Ernzerhof screened hybrid functional. *Journal of Chemical Physics*; 123(17): 1-8.

24. Dunning Jr, TH. 1989. Gaussian basis sets for use in correlated molecular calculations. I. The atoms boron through neon and hydrogen. *Journal of Chemical Physics*; 90(2): 1007-1023.

25. Nöth, H, Meister, W. 1961. Beiträge zur Chemie des Bors, VI: Über Subverbindungen des Bors. Hypoborsäure-tetrakis-dialkylamide und Hypoborsäure-ester. *Chemische Berichte*; 94(2): 509-514.

26. Tian, X, Goddard, R, Pörschkle, KR. 2006. (*β*-Diketiminato)palladium Complexes. *Organometallics*; 25(25): 5854-5862.

27. Allen, FH, Kennard, O, Watson, DG, Brammer, L, Orpen, AG, Taylor, R. 1987. Tables of bond lengths determined by X-ray and neutron diffraction. Part 1. Bond lengths in organic compounds. *Journal of the Chemical Society, Perkin Transactions 2*; 12: S1-S19.

28. Bernstein, J, Davis, RE, Shimoni, L, Chang, NL. 1995. Patterns in Hydrogen Bonding: Functionality and Graph Set Analysis in Crystals. *Angewandte Chemie International Edition*; 34(15): 1555-1573.

29. Spackman, MA, McKinnon, JJ. 2002. Fingerprinting intermolecular interactions in molecular crystals. *Crystal Engineering Community*; 4(66): 378-392.

30. Turner, MJ, MacKinnon, JJ, Wolff, SK, Grimwood, DJ, Spackman, PR, Jayatilaka, D, Spackman, MA. Crystal Explorer, Version 17.5, University of Western Avustralia, Pert, 2017.

31. Ece, A, Pejin, B. 2014. A computational insight into acetylcholinesterase inhibitory activity of a new lichen depsidone. *Journal of Enzyme Inhibition and Medicinal Chemistry*; 30(4): 528-532.

32. Koopmans, T. 1934. Über die Zuordnung von Wellenfunktionen und Eigenwerten zu den einzelnen Elektronen eines Atoms. *Physica*; 1(1-6): 104-113.